Chinese Chemical Letters 32 (2021) 3895–3898

Contents lists available at ScienceDirect

Chinese Chemical Letters

journal homepage: www.elsevier.com/locate/cclet

Communication

Visualizing nitric oxide-dependent HIF-1 activity under hypoxia with a lipid droplet-targeting fluorescent probe

Ying-Hao Pan, Xiao-Xiao Chen, Lei Dong*, Na Shao, Li-Ya Niu*, Qing-Zheng Yang

Key Laboratory of Radiopharmaceuticals, Ministry of Education, College of Chemistry, Beijing Normal University, Beijing 100875, China

ARTICLE INFO

Article history:
Received 12 March 2021
Revised 9 June 2021
Accepted 9 June 2021
Available online 15 June 2021

Keywords:
Bodipy
Fluorescent probe
HIF-1
Lipid droplet
Nitric oxide

ABSTRACT

Evaluating the correlation between hypoxia inducible factor 1 (HIF-1) and nitric oxide (NO) generated under hypoxia is of great significance. In this work, we developed a fluorescent probe for the monitor of HIF-1 activity influenced by NO under hypoxia in hepatoma cells with dual-targeting for hepatocyte and lipid droplet (LD). The probe shows excellent selectivity to NO and high sensitivity with 6000-fold fluorescence enhancement. Live cell imaging experiments revealed the probe's capability of imaging exogenous and endogenous NO with specific in LDs of HepG2 cells. For cells under hypoxia, HIF-1 induced LD level is observed to correlate with NO level. This work provides the *in-situ* visualization of NO-dependent HIF-1 upregulation through LD accumulation.

Liver cancer has become the second leading causes of cancer-related death worldwide, with growing numbers of new cases every year [1]. Hepatocellular carcinoma (HCC) consists of most liver cancers cases, mainly developed from the infection of hepatitis B and C virus, alcohol intake and so on. In the HCC region, cancer cells possess in a hypoxia environment due to the rapid growing of tumor and inefficient vasculature [2]. Under hypoxic condition, hypoxia inducible factor-1 (HIF-1) is overexpressed, regulating the growth and metastasis of HCC. Meanwhile, there are studies indicating that hypoxia mediated nitric oxide (NO) expression would correlate with HIF-1 expression [3,4]. NO and reactive oxygen species (ROS) are found to inactivate prolyl hydroxylases (PHDS), which is account for the hydroxylation and further degradation of HIF-1α. On the other hand, NO is also found to help stabilize HIF-1α through S-nitrosylation [5]. Thus, hypoxia-generated NO could help stabilize HIF-1α, consequently promote HIF-1 accumulation. However, studies on NO affecting HIF-1 expression have been mostly carried on from biological approach, mainly with western blot for HIF-1 expression. This approach could only provide *in vitro* result extracted from cells, which lacks original information from intracellular environment. *In-situ* visualization of NO affecting HIF-1 is still in demand for deep understanding of HIF-1 upregulation pathways.

Fluorescent probe is one of the most widely used techniques in cellular imaging for its noninvasive, highly sensitive and selective properties on real-time monitoring phenomenon *in-situ* [6,7]. It provides the opportunity to revealing the interactions between NO and HIF-1 in their native environments. However, because of the gaseous nature of NO and HIF-1 as a protein, the development of such probes that can simultaneously imaging these two factors is challenging. If a hallmark of HIF-1 can be imaged rather than directly imaging the protein, visualizing of both NO and HIF-1 by one probe could become achievable.

Lipid droplet (LD) is a subcellular organelle mainly considered as lipids and energy storage for cell growth. Since the rapidly proliferating cancer cells demand excess amount of energy, LD is found to be related in tumor cell activation and metabolism [8,9]. Studies have demonstrated that LD within the cells would accumulate under an HIF-1 dependent manner [10–12]. Under hypoxia, HIF-1 could upregulate lipogenic genes, activate lipin 1 or peroxisome proliferation activator receptor-α (PPARα), and suppress β-oxidation, which adds up to promote LD accumulation in cancer cells. Thus, evaluation of intracellular LD level could be a reasonable approach to assess HIF-1 activity [13]. Consequently, by monitoring the level of NO and LD simultaneously, visualizing NO influence on HIF-1 can be realized. Despite the development on fluorescent probe for NO [14–23] or LD [24–29] has advanced greatly in decades, imaging of NO in LD specifically for hepatocellular carcinoma has not been reported yet.

* Corresponding authors.
E-mail addresses: dl030131018@163.com (L. Dong), niuly@bnu.edu.cn (L.-Y. Niu).

https://doi.org/10.1016/j.cclet.2021.06.024
1001-8417/

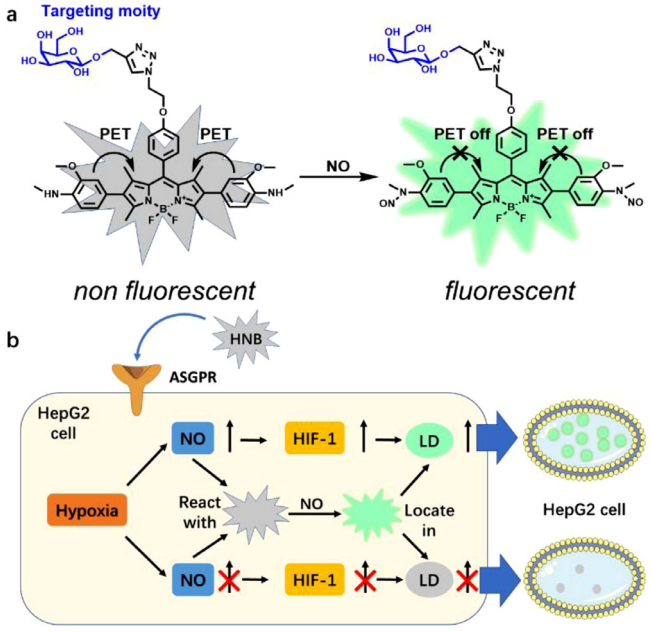

Scheme 1. (a) Proposed mechanism for HNB responding to NO and (b) schematic illustration of NO and HIF-1 induced LDs imaging by HNB targeting HepG2 cells.

Herein, we report a BODIPY-based LD and hepatocyte dual targeting fluorescent probe HNB for NO imaging, which is used for visualizing HIF-1 activity influenced by NO under hypoxia in HepG2 cells (Scheme 1). The probe utilizes 2–methoxy-*N*-methylaniline moieties as NO-reacting indicator. Fluorescence of HNB is quenched due to the photoinduced electron transfer (PET) effect from the two 2–methoxy-*N*-methylaniline moieties to the BODIPY core. After a nitrosation reaction of the electron-rich aromatic secondary amine with NO [30], fluorescence is recovered by inhibiting the PET process. Moreover, asialoglycoprotein receptor (ASGPr) is well known for its high expression on the surface of hepatocytes, which could recognize and bind galactose with high affinity. β-D-Galactose is attached to the BODIPY core by "click"-reaction, enabling the probe to target hepatocytes through ASGPr-mediated recognition and endocytosis. Finally, the non-polar HNB molecules automatically accumulate in LDs within the cells, realizing intracellular LD-targeting. With HNB, we evaluate the influence of endogenous NO on HIF-1 expression under hypoxia in HepG2 cells.

HNB was synthesizedby the route shown in Scheme S1 (Supporting information) and characterized by ^{1}H NMR, ^{13}C NMR spectroscopy and high-resolution mass spectrometry (HRMS). The optical properties of HNB responding to NO was investigated in a solution of PBS (pH 7.4, 10 mmol/L, containing 30 vol% CH_3CN). Under excitation at its maximum absorption of 530 nm (Fig. S1 in Supporting information), free HNB probe exhibited negligible fluorescence due to the PET effect from the 2–methoxy-*N*-methylaniline moieties to BODIPY core. Upon addition of DEA·NONOate (a commercial NO donor), the fluorescence of HNB raised drastically with a peak at 555 nm, and reached a plateau within 10 min (Fig. 1a). 10 equivalents of DEA·NONOate is sufficient to completely "turn-on" HNB (Fig. S2 in Supporting information), which gives an up to approximately 6000-fold intensity enhancement. Fluorescent titration of DEA·NONOate to 1 μmol/L HNB demonstrated a good linear relationship from 0 to 10 μmol/L (Figs. 1b and c) with a detection limit of 2.95 nmol/L ($S/N = 3$), which is below the physiological concentration of NO in cancer cells. The pH influence on NO detection was also conducted (Fig. S4 in Supporting information), which demonstrated that the fluorescence response to NO maintained sensitive in pH ranging from 4 to 9. Finally, we evaluated the selectivity of HNB to NO over other biological related molecules (Fig. 1d, Fig. S3 in Supporting information). None of metal ions, amino acids, reactive oxygen, sulfur and nitrogen

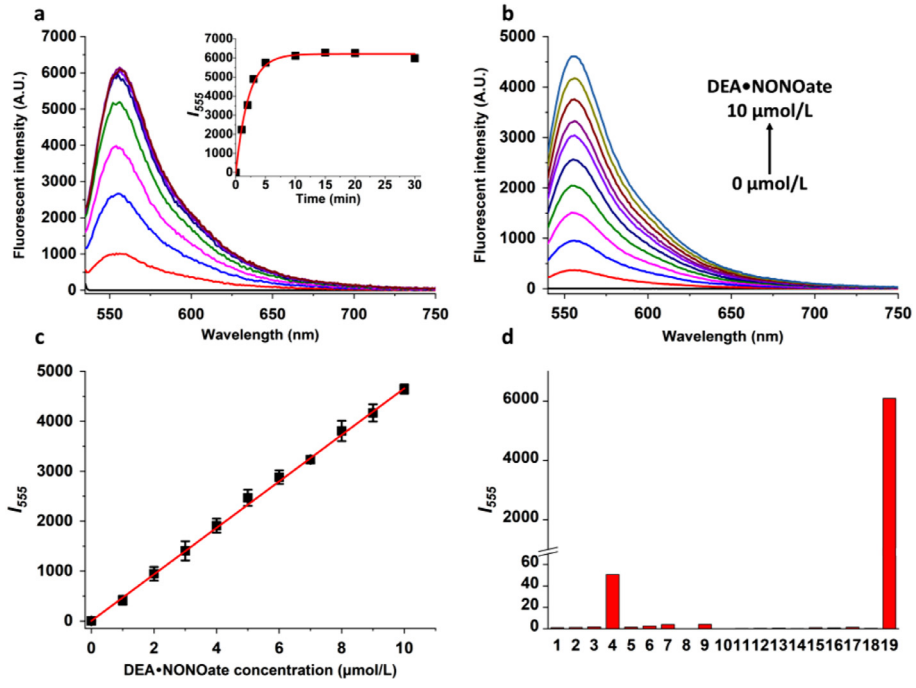

Fig. 1. (a) Time-dependent fluorescent spectra of 5 μmol/L HNB with 100 μmol/L DEA·NONOate, inset is the time-dependent fluorescent intensity at 555 nm. (b) Fluorescent response of 1 μmol/L HNB with 0–10 μmol/L DEA·NONOate for 30 min. (c) Linear relationship between the fluorescent intensity and DEA·NONOate concentration in (b), $R^2 = 0.9997$. (d) Fluorescent response of 5 μmol/L HNB upon addition of 20 equiv. of some major biological related molecules for 30 min, including blank (1), metal ions (2–7: Ca^{2+}, Cu^{+}, Cu^{2+}, Mg^{2+}, Fe^{2+}, Fe^{3+}), amino acids (8–12: Arg, Cys, Glu, His, Lys), ·OH (13), H_2O_2 (14), Hcy (15), GSH (16), H_2S (17), $ONOO^-$ (18) and NO (19). All fluorescent data was collected in PBS buffer (10 mmol/L, pH 7.4, containing 30 vol% CH_3CN) at 37 °C, $\lambda_{ex} = 530$ nm, $\lambda_{em} = 555$ nm.

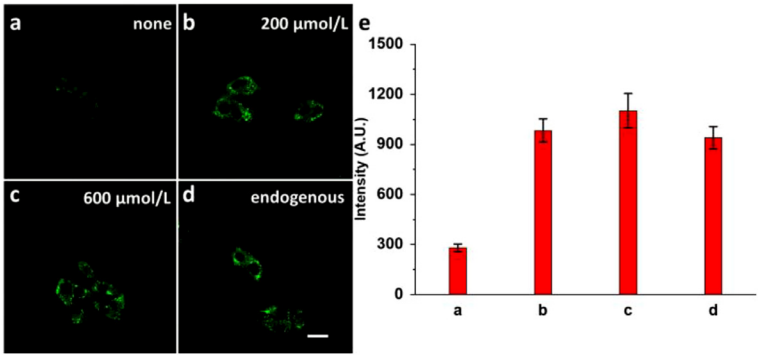

Fig. 2. Confocal fluorescence image of HepG2 cells (a-c) stained with 5 μmol/L HNB for 30 min, then treated with (a) 0, (b) 200 or (c) 600 μmol/L DEA·NONOate for another 30 min, (d) pretreated with 20 μg/mL LPS, 500 μg/mL L-Arg-and 0.01 μg/mL IFN-γ for 12 h, then treated with 5 μmol/L HNB for 30 min. (e) Fluorescent intensity in a-d, data was collected randomly in the cellular region. λ_{ex}: 487 nm, λ_{em}: 540–570 nm. Scale bar: 25 μm.

species could trigger fluorescent response, indicating the excellent specificity of HNB toward NO. The above-mentioned experiments in solutions demonstrated that HNB could detect NO with drastic fluorescence enhancement, fast response time and advantageous specificity under physiological conditions, which is suitable for further cellular study.

Before cellular imaging, cytotoxicity of HNB on targeting HepG2 cells was tested using CCK-8 assay (Fig. S5 in Supporting information). Negligible effect on cell viability was observed under 37 °C, indicating the good biocompatibility of HNB. Then, we evaluated whether it could detect exogenous and endogenous NO in human hepatocellular carcinoma cells (HepG2) cells with confocal laser scanning microscope (CLSM). When treated with NO donor DEA·NONOate for 30 min, much brighter fluorescence was observed in HepG2 cells than that without NO donor (Figs. 2a-c and e), which demonstrated HNB was capable of imaging exogenous NO. For endogenous NO imaging, lipopolysaccharide (LPS), L-arginine (L-Arg) and interferon-γ (IFN-γ) were used to induce iNOS expression according to literature [31] (Figs. 2d and e). After 12 h incubation, obvious fluorescence enhancement was detected comparing to untreated cells (Fig. 2a), indicating that HNB can image endogenous NO in HepG2 cells.

Then, we evaluated the recognition ability of HNB for HepG2 cells through ASGPr. For human cervical cells (HeLa), human non-small cell lung cancer cells (A549) and HepG2 cells treated with HNB and NO donor, only HepG2 cells emerged remarkable fluorescence comparing to HeLa and A549 cells, indicating the selective accumulation of HNB in HepG2 cells (Figs. 3a-c and g). To further confirm the selectivity attributes to the β-galactose mediated endocytosis of ASGPr, cellular uptake experiments of HNB with β-glucose or β-galactose were conducted (Figs. 3d-f and h). As the fluorescence of β-glucose co-incubated cells remain bright, distinct decrease on the fluorescence intensity of cells co-incubated with β-galactose was observed with increasing concentration of β-galactose. The decrease in fluorescence was attributed to the competition of β-galactose and HNB through ASGPr. Results above illustrated the ASGPr mediated HepG2 targeting ability of HNB.

In addition to the hepatoma targeting nature of HNB, its subcellular targeting capacity on lipid droplet was also evaluated. HepG2 cells were stained with HNB, Lipi-Blue (a commercial LD probe) and Lyso-tracker Deep red (a commercial lysosome probe), then treated with NO donor to determine the localization of HNB (Figs. 4a-e). As shown in Fig. 4, HNB colocalized well with LD probe Lipi-Blue, which had a Pearson's correlation of 0.85. Time-dependent confocal measurement further demonstrated the accumulation behavior of HNB in the LD region (Fig. S6 in Supporting information). Furthermore, LD accumulation induced by oleic acid was observed with HNB in the presence of NO donor (Fig. S7 in

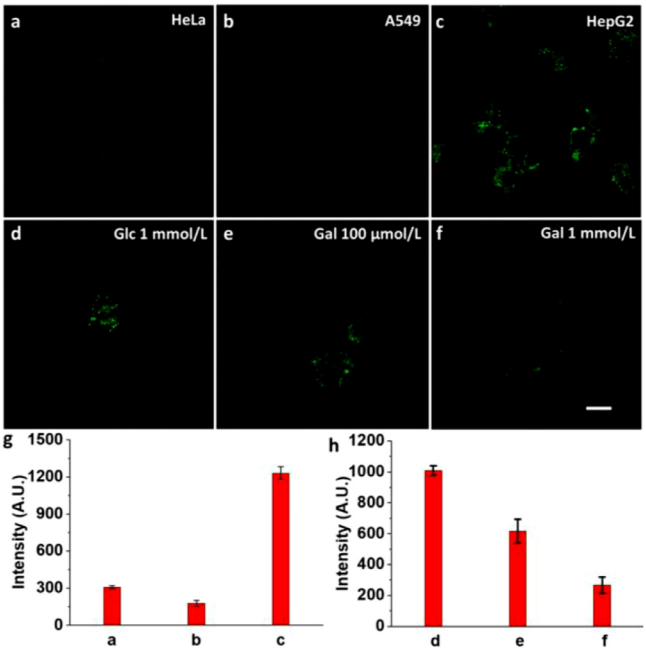

Fig. 3. (a-c) Confocal fluorescence image of (a) HeLa, (b) A549 and (c) HepG2 cells pretreated with 5 μmol/L HNB for 30 min, then treated with 200 μmol/L DEA·NONOate for another 30 min. (d-f) Confocal fluorescence image of HepG2 cells pretreated with 5 μmol/L HNB together with (d) 1 mmol/L β-glucose, (e) 100 μmol/L β-galactose or (f) 1 mmol/L β-galactose for 30 min, then treated with 200 μmol/L DEA·NONOate for another 30 min. (g) Fluorescent intensity in a-c, data was collected randomly in the cellular region. (h) Fluorescent intensity in d-f, data was collected randomly in the cellular region. λ_{ex}: 487 nm, λ_{em}: 540–570 nm. Scale bar: 25 μm.

Supporting information), which indicates that HNB is capable of monitoring cellular LD variation.

NO could be over-generated in tumor cells under hypoxia, and the NO level may correlate with HIF-1 expression in this condition. Since HIF-1 expression could be indicated by LD accumulation, we anticipate using HNB to image the relationship of NO and HIF-1 through LD level variation. HepG2 cells were cultured under hypoxia (2% O_2) for 6 h, then treated with HNB. Comparing to normorxic condition, high level of NO was observed with accumulation of LD within the cells (Figs. 5a and b). When NO scavenger PTIO or iNOS inhibitor L-NNA was added before hypoxia incubation, significant drop on fluorescent intensity was observed in obviously decreased amount LDs, indicating that both NO and LD level decreased (Figs. 5c and d). This phenomenon demonstrated that endogenously generated NO under hypoxia could promote HIF-1 upregulation. Furthermore, when HepG2 cells pre-

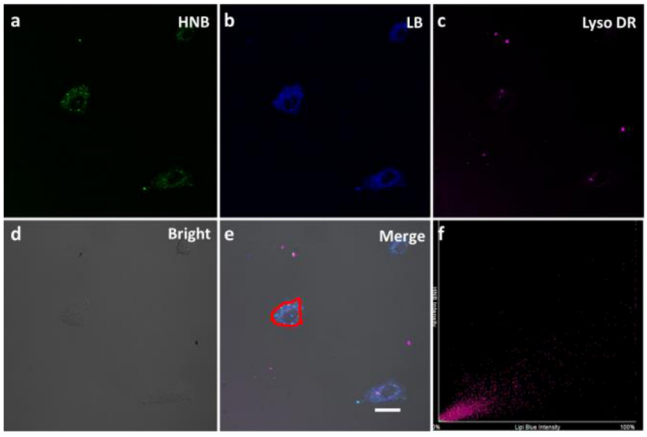

Fig. 4. Confocal fluorescence image of HepG2 cells: Treated with 5 μmol/L (a) HNB for 30 min, then treated with 200 μmol/L DEA·NONOate for 30 min, and then treated with 100 nmol/L (b) Lipi-blue and (c) 50 nmol/L Lyso-tracker deep red for 30 min; (d) Bright field and (e) merge; (f) Colocalization correlation was calculated for the red-circled area. Lipi-blue (LB) channel: λ_{ex}: 407, λ_{em}: 420–450 nm, HNB channel: λ_{ex}: 487 nm, λ_{em}: 540–570 nm, Lyso DR. channel: λ_{ex}: 638 nm, λ_{em}: 650–720 nm. Scale bar: 25 μm.

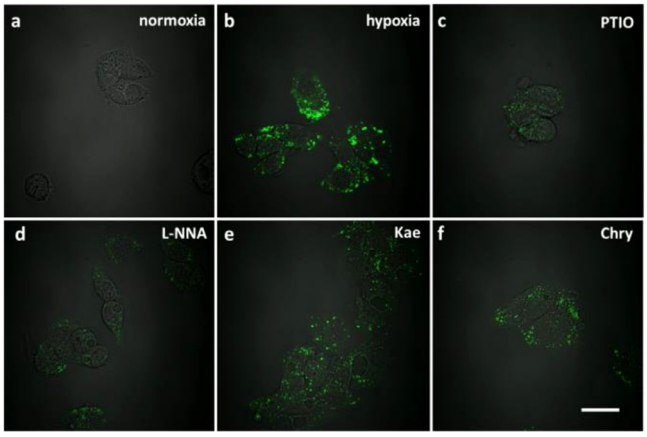

Fig. 5. Confocal fluorescence image of HepG2 cells: (a, b) Incubated in (a) normoxia condition (21% O_2) or (b) hypoxia condition (2% O_2) for 6 h, then treated with 5 μmol/L HNB for 30 min, (c-f) pretreated under hypoxia (2% O_2) with (c) 500 μmol/L PTIO, (d) 500 μmol/L L-NNA, (e) 50 μmol/L kaempferol or (f) 50 μmol/L chrysin, then treated with 5 μmol/L HNB for 30 min. λ_{ex}: 487 nm, λ_{em}: 540–570 nm. Scale bar: 25 μm.

treated with HIF-1 inhibitor kaempferol (Kae) or chrysin (Chry), cells were observed for lower LD level (Figs. 5e and f), while fluorescent intensity of NO in LDs maintained bright comparing to NO inhibited group (Figs. 5c and d), indicating generation of endogenous NO was not affected under hypoxia. To exclude NO generation from HIF-1 inhibitor, HepG2 cells were treated with kaempferol or chrysin under normoxia, in which endogenous NO were not observed (Fig. S8 in Supporting information). With the result above, we successfully visualized the NO-dependent HIF-1 upregulation in HepG2 cells under hypoxia. The results demonstrate that under hypoxic condition, NO is generated endogenously, and the overexpressed NO can trigger accumulation of LDs, indicating that NO could promote HIF-1 upregulation. This is the first time of visualizing NO-dependent HIF-1 upregulation with one fluorescent probe.

In conclusion, we have successfully developed a BODIPY-based glycosyl probe (HNB) for NO imaging, which has a dual-targeting ability to lipid droplets inside hepatocytes. The probe displayed excellent selectivity and sensitivity to NO. In the presence of NO, it exhibits an up to 6000-fold emission enhancement at 555 nm. Cell uptake and experiments proved that HNB is capable of targeting HepG2 cells through ASGPr-mediated endocytosis. Colocalization imaging illustrated that HNB could accumulate in LDs, which attributes to its non-polar nature. The probe can detect exogenous NO from donor and LPS/L-Arg/IFN-γ induced endogenous NO in living cells. Finally, HNB successfully imaged NO generation and HIF-1 expression through LD accumulation under hypoxia. With comparison of cells inhibiting NO generation or HIF-1 expression, we have visualized the HIF-1 upregulation with NO-dependent correlation with single probe for the first time. We hope that by providing intracellular *in-situ* information, this probe would help elucidate biological pathways involving variation of NO and LD levels.

Declaration of competing interest

The authors declare that they have no known competing financial interests or personal relationships that could have appeared to influence the work reported in this paper.

Acknowledgment

This work was financially supported by National Natural Science Foundation of China (Nos. 21971023, 22074007 and 21525206).

Supplementary materials

Supplementary material associated with this article can be found, in the online version, at doi:10.1016/j.cclet.2021.06.024.

References

[1] J.M. Llovet, J. Zucman-Rossi, E. Pikarsky, et al., Nat. Rev. Dis. Prim. 2 (2016) 16018.
[2] C.C.L. Wong, A.K.L. Kai, I.O.L. Ng, Front. Med. China. 8 (2014) 33–41.
[3] R. Chowdhury, L.C. Godoy, A. Thiantanawat, et al., Chem. Res. Toxicol. 25 (2012) 2194–2202.
[4] E. Martínez-Lara, A. Peña, J. Calahorra, A. Cañuelo, E. Siles, Food Funct. 7 (2016) 540–548.
[5] F. Li, P. Sonveaux, Z.N. Rabbani, et al., Mol. Cell. 26 (2007) 63–74.
[6] J. Zhang, X. Chai, X.P. He, et al., Chem. Soc. Rev. 48 (2019) 683–722.
[7] C. Yan, L. Shi, Z. Guo, W. Zhu, Chin. Chem. Lett. 30 (2019) 1849–1855.
[8] Q. Liu, Q. Luo, A. Halim, G. Song, Cancer Lett. 401 (2017) 39–45.
[9] P.T. Bozza, J.P.B. Viola, Prostaglandins Leukot. Essent. Fatty Acids 82 (2010) 243–250.
[10] I. Mylonis, H. Sembongi, C. Befani, et al., J. Cell Sci. 125 (2012) 3485–3493.
[11] S. Koizume, Y. Miyagi, Int. J. Mol. Sci. 17 (2016) 1–23.
[12] K. Bensaad, E. Favaro, C.A. Lewis, et al., Cell Rep. 9 (2014) 349–365.
[13] X. Shi, S.H.P. Sung, M.M.S. Lee, et al., Mater. Chem. B 8 (2020) 1516–1523.
[14] X.X. Chen, L.Y. Niu, Q.Z. Yang, Anal. Chem. 93 (2021) 3922–3928.
[15] X.X. Chen, L.Y. Niu, N. Shao, Q.Z. Yang, Anal. Chem. 91 (2019) 4301–4306.
[16] M. Yang, J. Fan, W. Sun, et al., Chem. Commun. 55 (2019) 8583–8586.
[17] C. Zhao, T. Zhu, N. Ren, et al., Angew. Chem. Int. Ed. 60 (2021) 8450–8454.
[18] M. Yang, J. Fan, J. Du, X. Peng, Chem. Sci. 11 (2020) 5127–5141.
[19] L. Teng, G. Song, Y. Liu, et al., J. Am. Chem. Soc. 141 (2019) 13572–13581.
[20] Y. Huo, J. Miao, L. Han, et al., Chem. Sci. 8 (2017) 6857–6864.
[21] Y. Huo, J. Miao, J. Fang, et al., Chem. Sci. 10 (2019) 145–152.
[22] P. Zhang, Y. Tian, H. Liu, et al., Chem. Commun. 54 (2018) 7231–7234.
[23] M. Ye, W. Hu, M. He, et al., Chem. Commun. 56 (2020) 6233–6236.
[24] H. Xu, H. Zhang, G. Liu, Anal. Chem. 91 (2019) 977–982.
[25] J. Gong, P. Wei, Y. Su, et al., Chin. Chem. Lett. 29 (2018) 1493–1496.
[26] K. Wang, S. Ma, Y. Ma, et al., Anal. Chem. 92 (2020) 6631–6636.
[27] J. Yin, M. Peng, W. Lin, Sens. Actuators B 288 (2019) 251–258.
[28] L. Guo, M. Tian, Z. Zhang, et al., J. Am. Chem. Soc. 143 (2021) 3169–3179.
[29] M. Collot, T.K. Fam, P. Ashokkumar, et al., J. Am. Chem. Soc. 140 (2018) 5401–5411.
[30] J. Miao, Y. Huo, X. Lv, et al., Biomaterials 78 (2016) 11–19.
[31] L.E. McQuade, J. Ma, G. Lowe, et al., Proc. Natl. Acad. Sci. U. S. A. 107 (2010) 8525–8530.